Accepted Manuscript

Impact of photochemical ageing on Polycyclic Aromatic Hydrocarbons (PAH) and oxygenated PAH (Oxy-PAH/OH-PAH) in logwood stove emissions

Toni Miersch, Hendryk Czech, Anni Hartikainen, Mika Ihalainen, Jürgen Orasche, Gülcin Abbaszade, Jarkko Tissari, Thorsten Streibel, Jorma Jokiniemi, Olli Sippula, Ralf Zimmermann

PII: S0048-9697(19)32465-9
DOI: https://doi.org/10.1016/j.scitotenv.2019.05.412
Reference: STOTEN 32573

To appear in: *Science of the Total Environment*

Received date: 19 March 2019
Revised date: 26 May 2019
Accepted date: 27 May 2019

Please cite this article as: T. Miersch, H. Czech, A. Hartikainen, et al., Impact of photochemical ageing on Polycyclic Aromatic Hydrocarbons (PAH) and oxygenated PAH (Oxy-PAH/OH-PAH) in logwood stove emissions, Science of the Total Environment, https://doi.org/10.1016/j.scitotenv.2019.05.412

Impact of photochemical ageing on Polycyclic Aromatic Hydrocarbons (PAH) and oxygenated PAH (Oxy-PAH/OH-PAH) in logwood stove emissions

Toni Miersch[a], Hendryk Czech[b,⍰,*], Anni Hartikainen[b], Mika Ihalainen[b], Jürgen Orasche[c], Gülcin Abbaszade[c], Jarkko Tissari[b], Thorsten Streibel[a,c], Jorma Jokiniemi[b], Olli Sippula[b,d], Ralf Zimmermann[a,c]

[a]*Joint Mass Spectrometry Centre, Chair of Analytical Chemistry, University of Rostock, Dr.-Lorenz-Weg 2, 18059 Rostock, Germany*

[b]*Fine Particle and Aerosol Technology Laboratory, Department of Environmental and Biological Science, University of Eastern Finland, Yliopistonranta 1, P.O. Box 1672, 70211 Kuopio, Finland*

[c]*Joint Mass Spectrometry Centre, Cooperation Group "Comprehensive Molecular Analytics" (CMA), Helmholtz Zentrum München,* Gmunder Straße 37, 81479 München*, Germany*

[d]*Department of Chemistry, University of Eastern Finland, Yliopistokatu 1, P.O. Box 111, 80101 Joensuu, Finland*

⍰*now at: Joint Mass Spectrometry Centre, Chair of Analytical Chemistry, University of Rostock, Dr.-Lorenz-Weg 2, 18059 Rostock, Germany*

**corresponding author: hendryk.czech@uni-rostock.de*

Abstract

The combustion of spruce logwood in a modern residential stove was found to emit polycyclic aromatic hydrocarbons (PAH) and oxygenated polycyclic aromatic hydrocarbons (OPAH) with emission factors of 404 µg MJ^{-1} of 35 analysed PAH, 317 µg MJ^{-1} of 11 analysed Oxy-PAH and 12.5 µg MJ^{-1} of 5 analysed OH-PAH, most of which are known as potential mutagens and carcinogens. Photochemical ageing in an oxidation flow reactor (OFR) degraded particle-bound PAH, which was also reflected in declining PAH toxicity equivalent (PAH-TEQ) values by 45 to 80% per equivalent day of photochemical ageing in the atmosphere. OPAH concentrations decreased less than PAH concentrations during photochemical ageing, supposedly due to their secondary formation, while 1-hydroxynaphthalene, 1,5-dihydroxynaphthalene and 1,8-naphthalaldehydic acid were significantly increased after ageing. Furthermore, secondary organic aerosol (SOA) formation and aromatic compounds not included in targeted analysis were investigated by thermal-optical carbon analysis

(TOCA) hyphenate to resonance-enhanced multi-photon ionisation time-of-flight mass spectrometry (REMPI-TOFMS).

The commonly used PAH-source indicators phenanthrene/anthracene, fluoranthene/pyrene, retene/chrysene, and indeno[cd]pyrene/benzo[ghi]perylene remained stable during photochemical ageing, enabling identification of wood combustion emissions in ambient air. On the other hand, benz[a]pyrene/benz[e]pyrene and benz[a]anthracene/chrysene were found to decrease with increasing photochemical age. Retene/chrysene was not a proper classifier for the wood combustion emissions of this study, possibly due to more efficient combustion than in open wood burning, from which this diagnostic ratio was initially derived.

This study motivates in-depth investigation of degradation kinetics of particle-bound species on different combustion aerosol as well as the consequences of photochemical ageing on toxicity and identification of wood combustion emissions in ambient air.

Keywords: toxicity equivalent, EC/OC, PEAR, diesel exhaust particles, photoionization mass spectrometry, wood combustion

Graphical Abstract

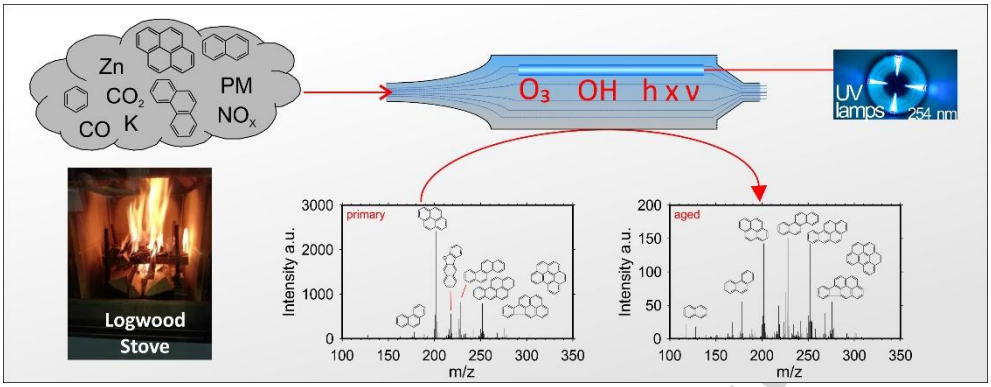

1. Introduction

Residential wood combustion has been identified as a substantial contributor to local air pollution at many sites in Europe (Cordell et al., 2016; Gaeggeler et al., 2008; Glasius et al., 2018; Hovorka et al., 2015; Qadir et al., 2014; Reche et al., 2012). The combustion of logwood in wood stoves can release high levels of toxic air pollutants, in particular if operated under stove overload (Bruns et al., 2015), low ratio of oxygen to fuel (Orasche et al., 2013), with high moisture content of logwood (Orasche et al., 2013) or if prolonged ignition phases occur (Czech et al., 2018). Wood smoke may induce toxicological effects in *in vitro* and *in vivo* models, such as DNA damage, cytotoxicity, inflammation and oxidative stress (Kanashova et al., 2018; Kasurinen et al., 2017; Naeher et al., 2007), and was assigned to group 2A ("probably carcinogenic to humans") by the International Agency of Cancer Research (IARC) (International Agency for Research on Cancer (IARC), 2019).

Among air pollutants such as carbon monoxide, benzene and black carbon (BC), polycyclic aromatic hydrocarbons (PAHs) and oxygenated PAHs (OPAHs = Oxy-PAHs + OH-PAHs) are emitted in the range of 0.1% - 1% of the total particulate matter (PM) released from logwood combustion. These compounds also include potent carcinogens, such as benzo[a]pyrene and dibenzo[ah]anthracene (Czech et al., 2018; Orasche et al., 2012). However, in the atmosphere primary aerosol undergoes chemical and physical transformation, which changes the toxicological properties of wood combustion emissions (Künzi et al., 2013; Nordin et al., 2015). The degradation of PAH is highly dependent on whether they exist in gaseous or condensed phase. On the one hand, gas phase PAH are efficiently oxidised in homogeneous reactions with OH radicals, O_3 and NO_3 radicals. On the other hand, heterogeneous reactions of particles-bound PAH with the same reactants are substantially slower and are affected by particle chemical composition and microstructure (Keyte et al., 2013). Previous studies demonstrated that second-order reaction constants of OH radicals and PAHs on kerosene flame soot (Bedjanian and Nguyen, 2010), graphite microparticles (Esteve et al., 2004), or diesel exhaust particle (Esteve et al., 2006), span the range of two orders of magnitude. In addition to chemical reactants, atmospheric degradation by photolysis and photo-initiated reactions is an

important pathway for particle-bound PAHs, but insignificant for gas phase PAHs (Vione et al., 2006). In contrast to PAHs, OPAHs are also produced by photochemical conversion of PAH precursors with ambiguous net production rate from complex multiphase chemistry (Walgraeve et al., 2010).

Oxidation flow reactors (OFRs) have been widely used to study aerosol ageing and secondary organic aerosol (SOA) formation from biogenic and anthropogenic volatile organic compounds (VOCs) as well as combustion emission sources (Ezell et al., 2010; Keller and Burtscher, 2012; Pieber et al., 2018) and ambient air (Palm et al., 2016; Tkacik et al., 2014). With high exposure of oxidising agents, OFRs enable extrapolation of atmospheric ageing up to several days within time scales of usually minutes in the photochemical reactors. Regarding chemistry, the recent modelling work on photochemical ageing in OFR indicates that relative importance of different non-OH reactants may be kept comparable to tropospheric VOC fate, despite the unnatural high oxidant exposure in OFRs (Peng et al., 2016; Peng and Jimenez, 2017).

In this study, we aged aerosol from the combustion of spruce logwood with recently introduced high-flow OFR "Photochemical Emission Aging flowtube Reactor" (PEAR) (Ihalainen et al., 2019). We investigated the fate of PAHs, Oxy-PAHs and OH-PAHs during photochemical aging and the effect of ageing on PAH diagnostic ratios for emission source identification. Moreover, carcinogenity of the emissions based on PAH toxicity equivalent (PAH-TEQ) (Nisbet and LaGoy, 1992) was determined and compared to emissions from a non-road diesel engine as reference for carcinogenic emissions "group 1" ("carcinogenic to humans") by IARC (International Agency for Research on Cancer (IARC), 2019).

2. Material and Method

2.1. Combustion appliances and fuels

Five consecutive batches of 2 kg of dry spruce wood (*Picea abies*) were burned in a modern non-heat-retaining chimney stove (*Aduro 1.1*, Denmark) featuring combustion air staging. The first batch was ignited top-down by using 150 g of spruce sticks as kindling and lasted for 35 min, whereas the

following four batches burned for 45 min. After the fifth batch, remaining ember was stoked and the secondary air supply channels were closed according to manufacture instructions for 30 min. The spruce logwood used in this study originates from two different suppliers and has slightly different composition (Table 1), which might explain differences in emissions. However, the differences in emissions between the two wood fuels were small and not significant at 5% (t-test for unequal variances) for CO, NMHC and the sums of PAH and OPAH. For the four ageing experiments described in the next section, only "spruce1" was used (Table 1).

The engine of this study was a EPA Tier 1/EU Stage II (equivalent to EURO 2) water-cooled 24.5 kW non-road diesel engine (*Kubota D1105-T*, 24.5 kW, 3000 rpm maximum speed, total displacement of 1123 cm^3) fuelled with Finnish summer grade ultra-low sulphur diesel (EN590 diesel fuel). The Finnish biodiesel content up to 7 vol-% consists of hydrotreated vegetable oil (HVO), therefore the oxygen content remains comparable to diesel fuel of fossil origin. Although equipped with a super glow system for shortening pre-heat time and quicker engine start-up in cold weather, the engine was always started about 30 min before measurements begun to enhance reproducibility. Engine settings comprise of four one-hour states including idling engine (Idle), intermediate 50 % with 39.92 Nm and 8.57 kW (IM50), rated 10 % with 7.07 Nm and 2.22 kW (R10), as well as rated 50 % with 35.55 Nm and 11.1 kW (R50), which were set and controlled by an Eddy current dynamometer system (Froude Consine Inc., MI, USA). In total, six experiments were conducted with the diesel engine.

Table 1 Physico-chemical properties (proximate analysis) of spruce logwoods

Property	Unit	spruce1	spruce2
Moisture	mass-%	8.3	7.6
C	mass-%	46.5	46.9
H	mass-%	5.8	5.8
O	mass-%	39.0	38.4
N	mass-%	< 0.05	< 0.05
S	mg kg^{-1}	60	110

K	mg kg^{-1}	568	912
Zn	mg kg^{-1}	12	39
ash	mass-%	0.44	1.2
Net heating value	KJ kg^{-1}	17620	17470
Net heating value (dry)	KJ kg^{-1}	19430	19110

2.2. Photochemical Emission Ageing flow tube Reactor (PEAR)

The Photochemical Emission Ageing flow tube Reactor (PEAR) belongs to the class of oxidation flow reactors for simulating atmospheric ageing within few minutes of processing. The PEAR basically consists of a stainless steel cylinder, covering a total volume of 139 L, and is equipped with four adjustable UV lamps (Osram, HNS 55W G13 HO; main emission at 254 nm, no emission at 185 nm). Externally fed ozone (4 ppm) is decomposed by the 254 nm radiation into O_2 and $O(^1D)$. The latter subsequently reacts with water vapour to form OH radicals. The temperature and relative humidity were set to 25°C and 50%, respectively, and controlled by HMP 110/65 (Vaisala, Finland). A total flow of 100 L min^{-1} gives a mean residence time of 62 s. Detailed descriptions of geometry, residence time distribution, flow profile, particle and vapour losses are given in Ihalainen et al. (2019).

All four ageing experiments were conducted at UV lamp voltage of 4x10 V equal to a photon flux of 2.99 10^{16} photons cm^{-2} s^{-1}, decreasing ozone concentration of 4 ppm to 1.9 ppm (Model 49i Ozone Analyser, Thermo Fisher Scientific Inc., MA, USA) in a blank experiment. Estimations of photochemical ages and importance of non-OH radical fate of VOC were done by Oxidation Flow Reactor (OFR) Exposure Estimator (v3.1) (https://sites.google.com/site/pamwiki/hardware/estimation-equations, (Peng et al., 2016). Data obtained from experiments with primary aerosol are consecutively denoted as “exp1p” to “exp4p” and corresponding aged aerosol as “exp1a” to “exp4a”.

2.3. Gas measurements

For wood combustion experiments, flue gases were led from the stove outlet to a stack placed below a hood. The stack draught was regulated by adjusting suction flow rate of the hood and with two

dampers placed in the stack. Regarding diesel engine experiments, flue gases were analysed after the tailpipe in the raw exhaust.

Gaseous emissions were continuously measured by Fourier-transform infrared spectroscopy with integrated O_2 analyser (DX-4000N, Gasmet Technologies Oy, Finland), directly from undiluted stack gas through an insulated and heated sampling line at 180 °C. Dilution for ageing experiments and filter sampling was controlled by monitoring CO_2 concentration (Carbocap GMP343, Vaisala, Finland) before and after a porous-tube/ejector dilutor (Venacontra, Finland). From the analysis of O_2 in the flue gas, emission factors (EFs) were calculated based on the instruction of the Finnish Standard Association method SFS 5624. Secondary EF were calculated in the same manner as primary EF, but using PAH, Oxy-PAH and OH-PAH concentration after ageing. Therefore, secondary EFs are always related to the equivalent of photochemical ageing and cannot be lower than zero by definition.

2.4. Filter sampling of PM2.5 and analysis

The aerosol emissions of the wood stove and the diesel engine were diluted at a dilution ratio of 30 or 15 and 10 or 8, respectively, by using a porous-tube/ejector dilutor (Venacontra, Finland) and cooled to room temperature to enable condensation of semi-volatile species. Subsequently, diluted primary emissions were segregated to an aerodynamic diameter smaller than 2.5 µm (PM2.5) and isokinetically sampled on quartz fibre filters (T293, Munktell, Sweden) over the total experiment duration of 4 h. Filter sampling after the PEAR was performed in the same manner, but with an additionally inserted ozone scrubber (Cordierite ceramic extrusion honey comb, BCE Special Ceramics GmbH, Germany) filled with KNO_2 (purity 97%, for analysis, ACROS Organics, NJ, USA) to prevent further oxidation of the sampled material. Finally, all filter samples were stored at −20 °C until analysis.

2.4.1. Thermal-optical carbon analysis hyphenated to resonance-enhanced multi-photon ionisation time-of-flight mass spectrometry (TOCA-REMPI-TOFMS)

The carbonaceous PM2.5 fraction was investigated by thermal/optical carbon analysis (TOCA) coupled to resonance-enhanced multi-photon ionisation time-of-flight mass spectrometry (REMPI-TOFMS) (Photonion GmbH, Germany) (Diab et al., 2015). A filter punch of 0.5 cm^{-2} was placed into the thermal-optical carbon analyser (DRI model 2001a) and analysed following the *ImproveA* protocol (Chow et al., 2007). During the four thermal subfractions of OC (OC1 to OC4) with upper temperature limits of 140 °C, 280 °C, 480 °C and 580°C, approximately 2% of the total flow enters the TOFMS through a deactivated transfer capillary (inner diameter of 200 µm), which is connected to the carbon analyser oven by a modified quartz cross (Grabowsky et al., 2011). In the ion source, UV radiation of 266 nm provided by the fourth harmonic generation of an Nd:YAG laser (*Big Sky Ultra*, Quantel, France; 20 Hz repetition rate, 1064 nm fundamental radiation, energy of 2 mJ at 266 nm) ionises selectively desorbed aromatic constituents of the particles in the REMPI process. In addition to the optical selectivity, REMPI at moderate laser intensity denotes a soft ionisation technique leading to predominantly molecular ions and low yields of fragments (Gehm et al., 2018). The generated ions were subsequently analysed by a TOFMS (*compact reflectron time-of-flight spectrometer II*, Stefan Kaesdorf Geräte für Forschung und Industrie, Germany) with unit mass resolution and a limit of detection of 10 ppb for toluene at 1 s time resolution. Finally, the obtained mass spectra intensities were summed up according to their occurrence in the four subfractions of OC.

2.4.2. In situ derivatisation thermal desorption gas chromatography mass spectrometry (IDTD-GCMS)

For targeted analysis, *in-situ* derivatisation direct thermal desorption gas chromatography time-of-flight mass spectrometry (IDTD-GCMS) with electron ionisation (Orasche et al., 2011) was applied to quantify 35 PAH, 11 Oxy-PAH and 5 OH-PAH bound on emitted PM (Fig. S1). Although 1,8-naphthaldehydic acid does not strictly belong to any of the three groups, it is here treated as OH-PAH for simplification. The *in situ* derivatisation is based on silylation with N-Methyl-N-trimethylsilyltrifluoroacetamide (MSTFA) during the step of thermal desorption from a quartz fibre

filter punch. Detected compounds were identified by library match of electron ionisation spectra as well as retention index and quantified by isotope-labelled internal standards of the same substance or chemically similar substances.

2.5. Data analysis

Statistical analyses by paired or unpaired Student's t-test with or without Welch-Satterthwaite modification for unequal variances and Levene's test for variance homogeneity were performed in Matlab (Version 2018b; The MathWorks Inc., MA, USA) using implemented functions from the Statistic Toolbox. In all hypothesis tests, the level of significance was set to 5%. If not otherwise stated, mean emission factors (EF) are given with one standard deviation as uncertainty.

3. Results and Discussion

3.1. Primary gases and VOC emissions from spruce wood combustion

Each of the single batches can be identified from the temporal evolution of main carbonaceous combustion gases CO_2, CO and non-methane hydrocarbons (NMHC) (Fig. 1). In the first batch, CO_2 features a bell-shaped temporal trend with a slow increase due to slow ignition and still relatively low temperature inside the firebox. When new logs are put onto glowing ember, the CO_2 concentration sharply increases to 9 % and steadily declines to 3 % during the combustion until the combustion procedure is repeated, while O_2 follows the inverse behaviour. Moreover, the majority of NMHC are released during the first few minutes after the ignition of a new batch, after which they levelled off below 50 ppm. CO follows the same concentration profile as NMHC, but with a substantial increase during the end of each batch when the wood has been converted into charcoal and secondary air supply channels were closed.

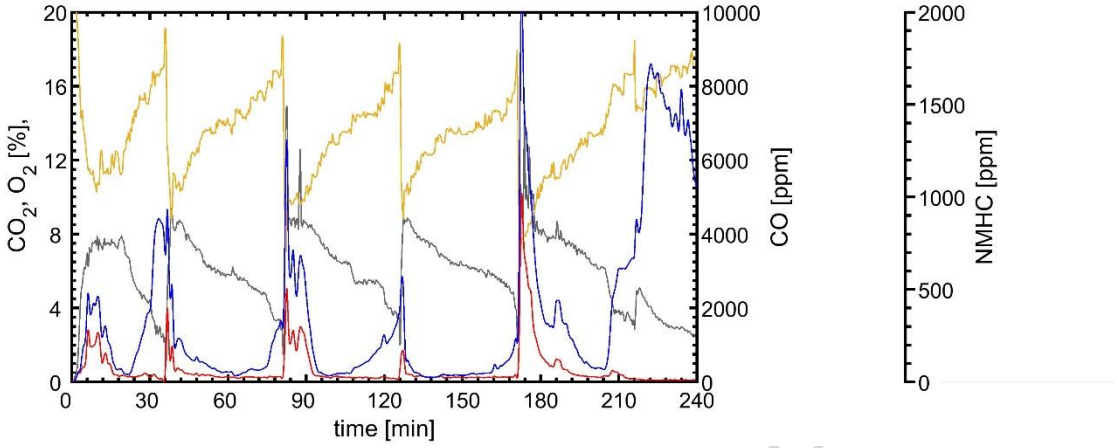

Fig. 1. Example of temporal concentration profiles of CO_2 (grey), O_2 (yellow), CO (blue) and non-methane hydrocarbons (NMHC, red) during five consecutive batches of spruce logwood combustion and final 30 min of char-burning.

Mean concentrations of CO_2, modified combustion efficiency (ΔCO_2 / (ΔCO + ΔCO_2)) and emission factors of single gases and VOC from the four hours combustion procedure are comparable to literature data of conventional wood stoves and appear between EFs of open fireplaces and heat-retaining modern masonry heaters (Czech et al., 2016; Evtyugina et al., 2014). Therefore, we regard the emissions described in this study as representative for European wood stoves. Furthermore, all emission factors of VOCs > 1 mg MJ^{-1} have lower coefficients of variation than 50%, so we assume that all combustion experiments followed the same concentrations profiles as exemplarily presented in Fig. 1.

Mean CO_2 and O_2 concentrations spanned the narrow range from 5.76 to 6.27% and 13.1 to 14.1%, respectively, while the CO emission was (2040 ±420) mg MJ^{-1}. The most abundant nitrogen-containing emission was NO with (35.5±3.7) mg MJ^{-1} followed by one order of magnitude lower EFs of NO_2, NH_3 and HCN (Table S1). The highest emission factor for volatile hydrocarbons was obtained for methane (34.6±9.9) mg MJ^{-1}, followed by benzene (26.0±4.1) mg MJ^{-1} and propene

(14.0±2.6) mg MJ^{-1}, accounting for 41% of the total detected VOC emissions. Formaldehydes denotes the oxygenated species with the highest mean EF of (6.7±1.8) mg MJ^{-1}.

3.2. Ageing conditions

The characterisation of gaseous and volatile primary emission constituents allows an estimation of the oxidation conditions inside the PEAR and an assessment of its comparison to ambient air. Two critical quantities are the ratio of photon flux to O_3 and external OH reactivity (OHR) to initial NO concentration. While the first one gives information about the non-OH fate of gases and VOCs including photolysis, ozonolysis and reactions with $O(^1D)$ and $O(^3P)$ (Peng et al., 2016), the second one determines the NO-condition and associated dominant radical chemistry (Peng and Jimenez, 2017). Here, in all experiments oxidation conditions can be classified as low-NO. In order to compare the PEAR to typical oxidation conditions in the troposphere, 'good', 'risky' and 'bad conditions' are adapted from Peng and Jimenez (2017) and depicted in Fig. 2. Oxidation conditions of this study mainly appear in the 'risky' range, but exceeds the limit to 'bad' oxidation conditions only shortly during the ignition of a new batch with OHR up to 10^4 s^{-1}. At such high OHR, the amount of available OH radicals for oxidation is significantly suppressed. Consequently, the resulting photochemical age during batch ignition accounts for only 0.2 days (assuming an average OH concentration of 10^6 molec cm^{-3}) (Prinn et al., 2001), but for 4-5 days on average during flaming phase with reduced OHR. Three of four combustion experiments with subsequent emission ageing led to mean photochemical ages of 1.7 days, whereas the one ageing experiment (exp3) produced aged aerosol with a significantly higher average photochemical age of 2.5 days. Emission factors for the four most important OH reactants butadiene, propene, CO and ethylene, which account for > 80% of the total OHR (Fig. S2), are entirely lower during the experiment of 2.5 days of ageing and may explain the difference.

Homogeneous gas phase reactions of volatile and semi-volatile PAHs in ambient air during daytime are usually dominated by OH radical chemistry. However, photochemical ageing of particle-bound PAH involves noticeable contribution from non-OH oxidising agents O_3 and NO_2. Furthermore, particle-bound PAH degradation is affected by their availability on the particle surface, the particle composition, and the impact of direct photolysis (Keyte et al., 2013). Under typical tropospheric oxidation conditions, O_3 and NO_2 can reach competitive importance in heterogeneous reactions compared to OH radicals (Keyte et al., 2013). However, ageing conditions in PEAR exhibit higher ratios of OH to O_3 and OH to NO_2 compared to ambient air. Thus, we continue assuming OH dominance over O_3- and NO_2-driven reactions.

From Peng and Jimenez (2017) we derive that during the major time of ageing, the primary aerosol was exposed to ”risky conditions” by means of a photon flux to OH exposure ratio $>10^7$ cm $^{s-1}$. Therefore, photolysis can be the dominating degradation mechanism, e.g. for toluene at OHR > 1800 s^{-1} during batch ignition. Although photolysis of gas phase aromatic hydrocarbons in the troposphere is negligible, direct photolysis may be important for particle-bound aromatic species (Vione et al., 2006). For single particle-bound aromatic compounds, an estimation cannot be made because of the unknown embedment of PAHs and OPAHs in the particle microstructure, light absorbing properties of other particle constituents and interaction with the particle constituents. For example, no trend was observed for single PAHs and OPAHs species in wood combustion and spark-ignition engine particles exposed to natural sunlight (Kamens et al., 1988; Kamens et al., 1989). In another study, the differences between the importance of photolysis for single aromatic species decreases with stronger absorption of visible and near-infrared light, which is associated with an increased content of soot (Behymer and Hites, 1988). Furthermore, it has been suggested that elemental carbon (EC) of combustion particles can initiate photooxidation through electron transfer on OC components and promote the generation of reactive species on the soot surface, leading to enhanced degradation of particle-bound organic compounds (Li et al., 2018). Although the emission spectrum of the UV lamps in this study covers blue to ultraviolet light and not the entire solar

spectrum, substantial radiation at about 440 nm might be relevant for the photochemical ageing as well (Li et al., 2018). Furthermore, it is possible that aromatic species are indirectly degraded by photosensitisers, which are produced or activated by radiation. For example, methoxy-phenols and -benzaldehydes, which are abundant and characteristic constituents of wood combustion aerosol, are suggested to enhance photodegradation of particle-bound aromatics (Vione et al., 2006).

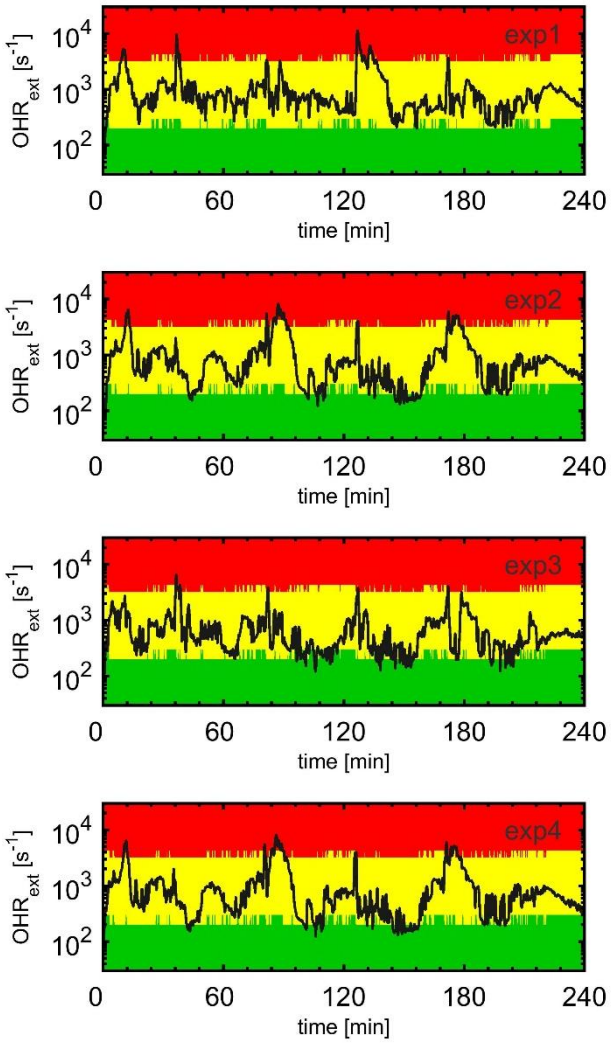

Fig. 2. External OH reactivity of the four combustion experiments with subsequent ageing with boundaries of 'good' (green), 'risky' (yellow) and 'bad' ageing conditions (red) according to Peng and Jimenez (2017).

3.3. Elemental (EC) and organic carbon (OC)

Fig. 3 illustrates the EF of elemental and organic carbon for all experiments as well as the gain in OC after ageing (secondary organic carbon, SOC). Primary emissions sampled at dilution ratios of 30 revealed (43±20) mg MJ^{-1} of EC and (9±6) mg MJ^{-1} of OC. OC results are comparable with previous studies of spruce logwood combustion of Czech et al. (2018) and Orasche et al. (2012). In contrast, EC values were substantially higher by a factor of four and three respectively, which might be caused by different combustion technologies. Eventually, the resulting ratio of OC to EC (OC/EC) for the experiments with a dilution factor of 30 was 0.21±0.04. Such low OC/EC ratios have been usually associated with traffic emissions or fossil fuel burning (Pio et al., 2011). However, recent studies indicate that some modern small and mid-scale wood combustion appliances emit particulate carbon with OC/EC ratios distinctly lower than unity (Kortelainen et al., 2015; Lamberg et al., 2013; Nuutinen et al., 2014; Sippula et al., 2017).

In exp3, 40% less EC (30mg MJ^{-1}) and 50% less OC (4±1 mg MJ^{-1}) was emitted, leading to an OC/EC of 0.14±0.02. The divergent behaviour of exp3 was in accordance with the higher modified combustion efficiency and lower mean CO concentration, which was 33% lower than in the other experiments. Hence, we conclude that exp3 featured fast ignition and better burning conditions than other experiments.

Photochemical ageing increased OC by 32%, 43 %, 39% and 26% for exp1 to exp4, respectively. For exp1, exp2 and exp4, EC decreased by less than 2%, whereas in exp2 EC declined by almost 10%. Although the correction of wall losses in smog chamber experiments is often conducted based on BC, we decided against this method deploying EC for three reasons. Firstly, the particle wall losses in the PEAR, determined by using silver particles, were found below 2% (Ihalainen et al., 2019). Secondly, the split between OC and EC based on optical correction laser transmittance / laser reflectance can be determined with 5-10% precision. Finally, EC might also change its optical properties during ageing, which would bias the optical correction.

It must be mentioned, that inorganic carbon (IC), i.e. carbonates, was not considered in this study, which may lead to biased carbon fraction results. IC is classified as OC or EC, depending on the decomposition temperature of the individual inorganic salt, and can account for up to 10% of total carbon in batchwise wood combustion (Lamberg et al., 2011).

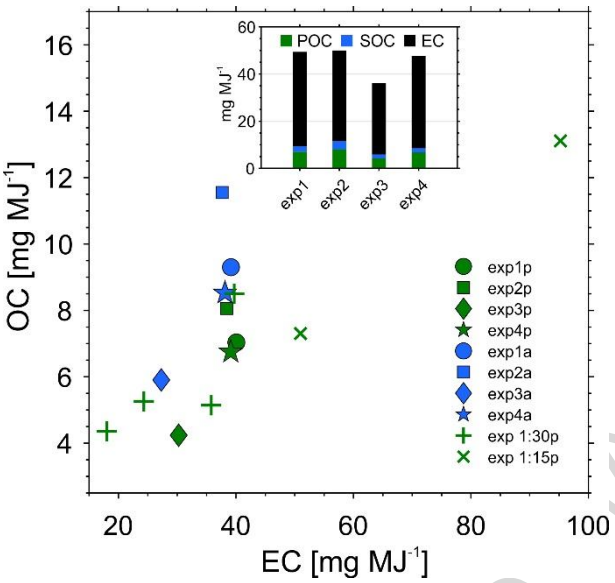

Fig. 3. Emission factors of organic (OC), primary organic (POC), secondary organic (SOC) and elemental carbon (EC) for primary and aged spruce combustion aerosol. For exp1 to exp4, both primary ("p", green) and aged ("a", blue) particles were analysed while "+" and "x" denote further combustion experiments with only primary particle sampling at dilution ratios of 30 and 15, respectively.

3.4. Untargeted analysis of aromatic PM constituents

By hyphenation of resonance-enhanced multi-photon ionisation time-of-flight mass spectrometry (REMPI-TOFMS) to thermal/optical carbon analysis (TOCA), the aromatic fingerprint of each single thermal fraction can be rapidly obtained and without any sample preparation. The first two fractions (OC1+OC2) from *ImproveA* protocol were combined due to the assumption that up to 280°C organic

compounds mainly evaporate without substantial decomposition. The last two OC fractions (OC3+OC4) were conflated as pyrolysis-like fraction OC34, in which mass spectra are characteristically shifted towards lower m/z due to decomposition of low-volatile organic compounds (Diab et al., 2015).

Most abundant peaks in the mass spectra of primary particles (Fig. 4, left) can be attributed to pyrene/fluoranthene (m/z 202), benzo[a]anthracenes/chrysene (m/z 228) and benzopyrenes (m/z 252), which are also labelled with their homologue alkylation series (m/z +14). Peaks of OPAH, such as naphthol (m/z 144), naphthoquinone (m/z 158), anthraquinone (m/z 208), benzonaphthofurans (m/z 218) and benzanthraquinone (m/z 258) were observed, even when their intensities were up to three orders of magnitude lower than the signal of the respective PAH core structure. The assignment of single structures in the higher mass range (m/z 300 - 400) was not possible based on unit mass, but due to the ionisation selectivity of REMPI at 266 nm we can assume at least one aromatic ring. Detected signals at m/z 308, 318 and 344 might stem from lignans, PAH, PAH-derivatives or thermal alteration products of di- and triterpenes (Czech et al., 2018). In this context, it should be mentioned that absolute intensities in the spectra do not reflect the absolute composition due different photoionisation cross sections, which may differ between up to two orders of magnitude (Gehm et al., 2018). As already discussed in the former section, the experiment exp3 showed a different mass spectrometric pattern and 50 to 80% lower abundancies for primary emission.

The parent PAH in a homologue series always stands for the most intense peak with declining intensities towards a higher degree of alkylation. An exception of this finding denotes the alkylated series of phenanthrene, where C4-phenanthrene showed 5-times higher peak intensity than C3-phenanthrene. This can be reasoned by the formation of retene (m/z 234) by the thermal alteration of diterpenoids in the resin of spruce wood (Simoneit, 2002).

During ageing, the intensities of all detected species decreased significantly (Fig. 4, right), which is in accordance with the results of the targeted PAH and OPAH analysis of the subsequent section. The

abundance of particle-bound pyrene/fluoranthene (m/z 202) and methylated derivatives (m/z 216) were reduced by 95%, while chrysene/benzo[a]anthracene (m/z 228) as well as their methylated derivatives (m/z 242) were detected with 80-90% lower intensity than in the primary emissions. Benzopyrenes (m/z 252) and C1-benzopyrenes (m/z 266) decreased by approximately 80%.

Exp3 revealed higher PAH reduction rates due to the longer photochemical age of approximately 2.5 days in contrast to 1.7 days of the experiments exp1a, exp2a and exp4a. For example, pyrene/fluoranthene was reduced by 98% and C1-pyrene/-fluoranthene on the aged particles appeared below the limit of detection. The 95% reduction of benzo[a]anthracene/chrysene is also higher in exp3 than in the experiments of 1.7 days of photochemical ageing. However, the ratio of single PAH concentration in primary and aged particles may differ to that obtained from targeted analysis in the following section because isobaric compounds cannot be separated only by their m/z.

The REMPI mass spectra of the pyrolysis fractions (OC3+OC4) of the primary emissions (Fig. S3, left) were dominated by lower masses, which originated from the thermal degradation of low-volatile organic compounds and belong predominantly to parent PAH and OPAH. Most abundant peaks can be assigned to naphthalene (m/z 128), phenanthrene (m/z 178), pyrene (m/z 202), benzo[a]anthracenes/chrysene (m/z 228) and benzopyrenes (m/z 252). However, also aromatic species of higher molecular weight such as benzo[ghi]perylene (m/z 276), coronene (m/z 300), dibenzo[ae]pyrene (m/z 302) or dibenzo[cdlm]perylene (m/z 326), which are incompletely volatilised at 280°C in OC2, can be detected.

The pyrolysis-like fraction OC34 of the aged particles (Fig. S3, right) showed a very similar pattern to OC34 of the primary combustion aerosol, but with generally lower intensities. Also in OC34, exp3a generally exhibits lower abundancies than ageing experiments with 1.7 days of photochemical age. Nevertheless, m/z 94, 118, 144 and 166 increased by 10 to 200% in two or three experiments of 1.7 days of photochemical age. These m/z values can possibly be assigned to oxygenated aromatics, such as phenol (m/z 94), benzofuran (m/z 118), naphthol (m/z 144) and esters of methoxybenzoic

acid (m/z 144, m/z 166), which may result from the thermal decomposition of larger aged organic aerosol constituents.

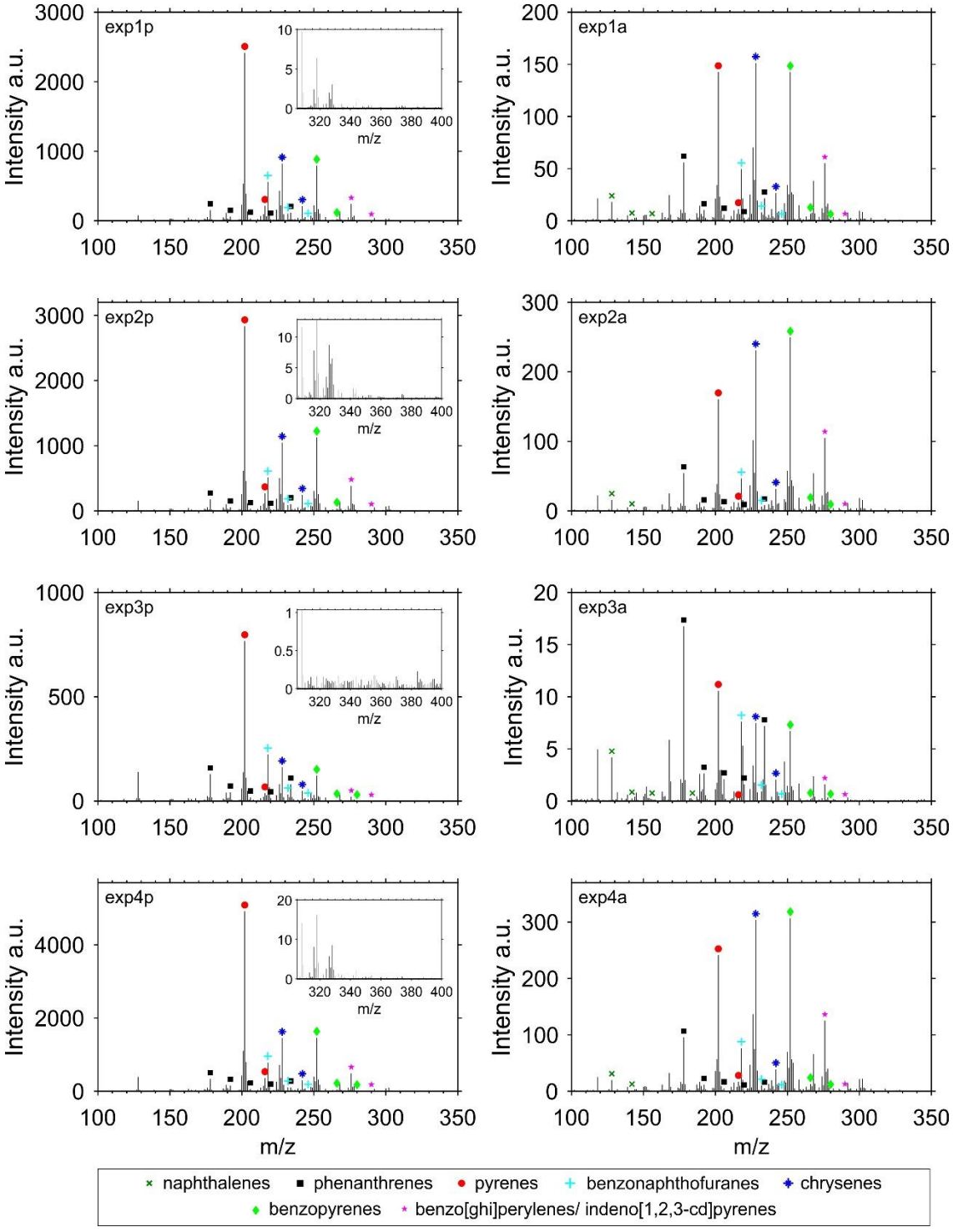

Fig. 4. Summed REMPI mass spectra during OC1 and OC2 (from room temperature to 280°C) of primary spruce combustion aerosol (left) and corresponding aged aerosol (right).

3.5. Targeted analysis of PAHs, Oxy-PAHs and OH-PAHs

3.5.1. Emission factors

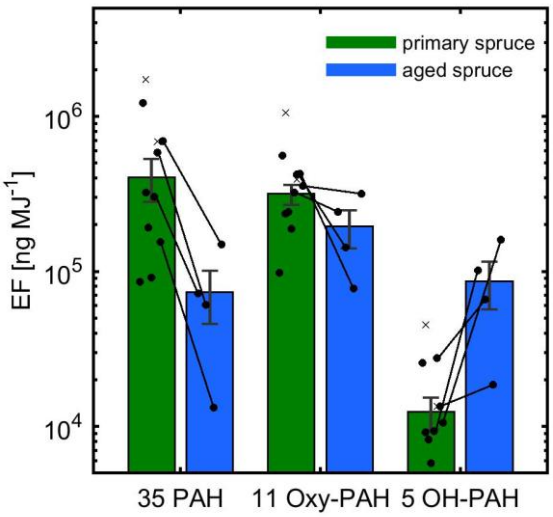

Fig. 5. Mean emission factors (EF) of total analysed PAHs, Oxy-PAH and OH-PAH in primary (n = 9) and aged spruce combustion aerosol (n = 4) with standard error of the mean (s.e.m.). Black circles denote dilution factor of 30, black crosses dilution factor of 15 (not included in mean calculation). Black lines show connection between primary and aged aerosol EF of the same experiment. See Table S3 for details.

From the targeted analysis of 35 PAH, 11 Oxy-PAH and 5 OH-PAH (Table 2), total EF of 404 µg MJ^{-1}, 317 µg MJ^{-1} and 12.5 µg MJ^{-1} were obtained, respectively (Fig. 5). Furthermore, the order of magnitude of the four most abundant PAH fluoranthene, pyrene, chrysene and benzo[ghi]fluoranthene, as well as dominant OPAH fluorenone and naphthalic anhydride are typical for organic wood combustion emissions. However, in particular because the majority of the targeted aromatic emissions from wood combustion are semi-volatile three- and four-ring-PAH and two- and

three-ring-OPAH, the sampling procedure may affect the gas-particle partitioning and consequently the EF of particle-bound PAH and OPAH. In two additional experiments with dilution factor of 15 instead of 30, highest and third highest EF out of 11 EF for were observed. Moreover, the combustion of solid fuels in general and changes in combustion conditions increase variances in EF even with similar combustion technology, e.g. partially closed air inlets may increase especially PAH emissions (Orasche et al., 2013). Therefore, EF of PAHs and OPAHs in the same order of magnitude can be regarded as comparable to previously reported EF for common wood stoves fuelled with spruce logwood (PAH: 126 µg MJ^{-1}, Oxy-PAH: 88.6 µg MJ^{-1} (Nyström et al., 2017); PAH: 319 µg MJ^{-1}, Oxy-PAH: 533 µg MJ^{-1} (Orasche et al., 2012); PAH: 126 µg MJ^{-1} (Avagyan et al., 2016)). EF of total OH-PAHs appear lower than in the literature (OH-PAH: 82.8 µg MJ^{-1} (Avagyan et al., 2016)), most likely to due to different selection of analytes and high dependence on burning conditions. Furthermore, EF of primary emissions from the four combustion experiments with subsequent ageing appear within the range of total PAH and OPAH EF of five combustion experiments at dilution of 30 without ageing, thus being also representative for the entire combustion experiment series.

Photochemical processing of four wood combustion experiments revealed significant decrease in PAHs, expressed as secondary EF for 1.7 to 2.5 days of photochemical ageing in the atmosphere. Apart from phenanthrene and anthracene, all detected PAH were degraded by 37% to 99%. Anthanthrene, acephenanthrylene, retene, perylene, and benz[a]pyrene were most affected by photochemical ageing, whereas unknown PAH#2 of m/z 302, unknown PAH#1 of m/z 302, coronene, benz[e]pyrene and naphtho[1,2-kb]fluoranthene were most stable. However, for some PAH degradation by ageing could not be properly determined because of concentrations below the limit of quantification. Despite different ageing conditions and particle compositions between different experiments, benz[a]pyrene appears consistently the most reactive PAH amongst the PAHs with more than four aromatic rings (Esteve et al., 2006; Jariyasopit et al., 2014). Additionally, benzo[e]pyrene and PAHs with more than five rings show consistently slower degradation, in agreement with previous studies (Jariyasopit et al., 2014; Walgraeve et al., 2010). Consequences of

these findings for carcinogenic effects of aged aerosol and emission source identification are discussed in the following sections.

To normalise the degradation of PAHs per photochemical day for each experiment, we estimated pseudo-first order rate constants k under constant exposure to oxidising agents (Fig. S4). Coefficients of variation (CoV) for k of each targeted PAH show values between 11% and 66% with a mean CoV of 34%, demonstrating that ageing experiments were repeatable and the majority of variance results from variation in primary emissions. Furthermore, CoVs for each targeted analyte remain almost constant comparing primary and aged particles, hence variances mainly arise from the combustion itself.

Although fewer OPAH than PAH were analysed, EF of PAH and Oxy-PAH were not significantly different, highlighting wood combustion as an important source of OPAHs in ambient air. Among 11 analysed Oxy-PAHs, naphthalic anhydride was the most abundant aromatic compound and accounted for 42% of the total Oxy-PAHs, similar to previously reported emissions from spruce logwood combustion (Orasche et al., 2012). In contrast to airborne PAHs, which are assumed to be predominantly formed in combustion processes, Oxy-PAHs may originate from both primary sources and from atmospheric ageing of PAHs and other precursors (Walgraeve et al., 2010). In fact, Oxy-PAHs concentration decreased less than those of PAH and even revealed a net increase for benz[a]anthracen-7,12-dione in two of the four ageing experiments, which emphasises the presence of a source counteracting the photochemical sink.

OH-PAHs were less abundant than PAH and Oxy-PAH in primary PM, but increased after photochemical ageing. In particular, for 1-hydroxynaphthalene, 1,5-dihydroxynaphthalene and 1,8-naphthaldehydic acid the photochemical source dominated the photochemical sink in all experiments with average enhancement ratios of 3, 13 and 36, respectively. OPAHs are regarded to be more toxic than their PAH counterpart due to unnecessary enzymatic activation for direct mutagenic potential (Fu et al., 2012) and might be a significant contributor to toxicity of aged aerosol or ambient PM.

Table 2 Mean emission factors (EF) and standard deviation (s.d.) of PAHs, Oxy-PAHs and OH-PAHs emissions for primary spruce logwood combustion (n = 9) and aged spruce logwood combustion (n = 4) in [ng MJ^{-1}].

	Spruce primary		Spruce aged	
	Mean	s.d.	Mean	s.d.
Phenanthrene	10000	9740	4710	2640
Anthracene	2260	2080	764	575
Fluoranthene	64400	59500	7690	5320
Acephenanthrylene	15800	15200	301	187
Pyrene	56200	51400	4630	3260
Benzo[c]phenanthrene	4380	3860	706	604
Benzo[ghi]fluoranthene	31800	29500	6640	5670
Benz[a]anthracene	17900	16500	1430	1340
Chrysene	30000	25400	7450	6320
ΣBenzo[b,k]fluoranthene	52600	47700	12700	10000
2,2''-Binaphthalene'	3400	3050	619	606
Benz[e]pyrene	36400	36200	11400	8580
Benz[a]pyrene	10600	10700	515	413
Perylene	2910	2950	114	78.1
Anthanthrene	843	1010	14.5	14.5
Dibenz[ah]anthracene	1010	1060	213	168
Indeno[1,2,3-cd]pyrene	6500	6500	1820	1510
Picene	1000	1000	290	269
Benzo[ghi]perylene	14400	14900	3710	2950
Coronene	5570	6120	1650	1310
Retene	4400	2040	140	120

unknown PAH m/z 302 #1	252	249	96.5	70.8
unknown PAH m/z 302 #2	201	207	66.7	45
Naphtho[1,2-kb]fluoranthene	6670	6630	1980	1740
Dibenz[al]pyrene	4430	4320	1210	1050
Naphtho[2,3-b]fluoranthene	4230	4160	939	803
Dibenz[ae]pyrene	1460	1510	311	241
Naphtho[2,1-a]pyrene	2180	2900	278	420
Naphtho[2,3-a]pyrene	1720	2000	533	698
Dibenz[ai]pyrene	684	806	<10	-
Dibenz[ah]pyrene	357	379	<10	-
9-Methylphenanthrene	320	409	<3.5	-
4-Methylpyrene	2000	1710	121	105
2-Methylpyrene	3610	3150	305	270
1-Methylpyrene	3670	3230	235	206
9H-Fluoren-9-one	52500	58000	13800	4400
9,10-Anthracenedione	26400	15000	17100	7850
Cyclopenta(def)phenathrenone	28400	23200	4070	2520
1,8-Naphthalic anhydride	132000	53000	128000	72200
11H-Benzo[a]fluoren-11-one	10200	7760	2890	2030
7H-Benzo[c]fluorene-7-one	3530	2570	999	693
11H-Benzo[b]fluoren-11-one	12500	9480	4470	3210
7H-Benzo[de]anthracen-7-one	30000	25500	13000	10000
Benz[a]anthracene-7,12-dione	1880	1320	1480	977
5,12-Naphthacenedione	1210	1270	867	629
Xanthone	18100	8450	7540	3030

1-Hydroxynaphthalene	1070	787	3430	1640
2-Hydroxynaphthalene	2600	2010	2790	1420
1,8-Dihydroxynaphthalene	5260	2730	5560	2500
1,5-Dihydroxynaphthalene	667	629	4130	2400
1,8-Naphthalaldehydic acid	2880	4560	70600	52500

3.5.2. Reassessing PAH diagnostic ratios in primary and aged wood combustion aerosol

Table 3 Comparison of PAH diagnostic ratios from primary (n = 11) and aged wood combustion emissions (n = 4) with literature values (Galarneau, 2008; Ravindra et al., 2008; Tobiszewski and Namieśnik, 2012)

diagnostic ratio	PAH source	Galarneau 2008[a]	Tobiszewski & Namieśnik 2012	primary[b]	aged[b]
PHE / (PHE+ANT)	wood combustion	0.68 - 1.00	-	0.72 - 0.92	0.83 - 0.92
FLA / (FLA+PYR)	wood combustion	0.35 - 0.67	>0.5	0.51 - 0.57	0.61 - 0.64
BaA / (BaA+CHR)	wood combustion	0.34 - 0.84	-	0.31 - 0.41	0.14 - 0.21
IcdP / (IcdP+BghiP)	wood, biomass and coal combustion	0.40 - 0.76	>0.5	0.67 - 0.70	0.66 -0.69
BaP / (BaP+BeP)	photochemically aged particles	-	<0.5	0.16 - 0.31	0.03 - 0.06
RET / (RET+CHR)	combustion coniferous wood	-	~1	0.03 - 0.25	0.00 - 0.15

PHE = phenanthrene, ANT = anthracene, FLA = fluoranthene, PYR = pyrene, BaA = benz[a]anthracene, CHR = chrysene, IcdP = Indeno[cd]pyrene, BghiP = Benzo[ghi]perylene, BaP = benz[a]pyrene, BeP = benz[e]pyrene, RET = retene.

[a]standard deviation

[b]minimum - maximum

Ratios of different PAH or PAH isomers have been used to estimate the dominant emission sources in ambient aerosol as well as in water and soil (Tobiszewski and Namieśnik, 2012). However, due to large variances in emissions and especially different reactivities of PAH species in the atmosphere, this concept has been widely criticised (Galarneau, 2008; Ravindra et al., 2008). In the application of six common PAH diagnostic ratios, found in Tobiszewski and Namiesnik (2012) and Galarneau (2008), on the primary and aged spruce combustion aerosol, three diagnostic ratios turned out to give the correct classification without constraints (Table 3). Diagnostic ratios from phenanthrene and anthracene, fluoranthene and pyrene, and indeno[cd]pyrene and benzo[ghi]perylene occurred within the expected ranges with only minor effects from photochemical ageing. Considering the different reactivity of phenanthrene and anthracene in homogeneous reaction with OH radicals, the phenomenon of protection of particle-bound PAHs by the particle matrix towards oxidation (Keyte et al., 2013) seems to dominate the photochemical degradation despite significant abundancies in the gas phase for both semi-volatile PAH species (Keyte et al., 2016). However, photolysis may play an important role for PAH degradation, in particular during the ignition of a new batch of logwood when high levels of PAHs along wisth organic aerosol are released (Eriksson et al., 2014). Although significant differences in means (paired-sample t-test with Dunn-Sidak correction, significance level of 5%) were observed for the diagnostic ratio of fluoranthene and pyrene, it is still located in the expected range for wood combustion aerosol. Benz[a]anthracene and chrysene also provide correct classification, although very closely at the limit suggested by Galarneau (2008). On the other hand, aged spruce combustion aerosol appears clearly outside the range. Therefore, the diagnostic ratio of benz[a]anthracene and chrysene must be regarded as an appropriate classifier only for fresh wood combustion emissions, whereas phenanthrene and anthracene as well as fluoranthene and pyrene allows identification of wood combustion as source even after approximately one day of photochemical ageing.

The diagnostic ratio of benz[e]pyrene and benz[a]pyrene were suggested to distinguish between fresh and photochemically aged combustion emissions (Tobiszewski and Namieśnik, 2012).

Apparently, diagnostic ratios of primary emissions in this study are already outside the suggested range, likely because the data used to derive this diagnostic ratio limited the validity to traffic emissions (Oliveira et al., 2011). However, benz[e]pyrene and benz[a]pyrene clearly enable monitoring of the photochemical ageing of wood combustion emissions due to their substantial difference in reactivity towards OH radicals, sunlight and ozone (Keyte et al., 2013; Ravindra et al., 2008).

The diagnostic ratio of retene and chrysene involves analytes encompassing the backbone of di- and triterpenoids in the wood. During combustion, di- and triterpenes are thermally degraded by elimination of side chains and functional groups and form retene and chrysene. From the thermal decomposition (pyrolysis) of resinoic acids, a variety of other products with both higher and lower degree of substitution than retene is known (Fine et al., 2004). On the other hand, chrysene can be formed by pyrolysis of triterpenoids as well, but also by the radical mechanism hydrogen-abstraction-carbon-addition (Ravindra et al., 2008). The emission of these species follows different formation mechanisms, thus combustion conditions such as fuel bed temperature and air supply likely play a role, along with the varying resin content of different coniferous wood species (Nuopponen et al., 2006). Furthermore, the proposed diagnostic ratio was derived from analysis of cores from lake sediment in New York (NY, USA) in order to examine emission sources during approximately the past 100 years (Yan et al., 2005). In fact, data of fireplace emissions from the combustion of spruce and pine revealed diagnostic ratios >0.9 (Fine et al., 2004), but emissions from present day wood stoves do not seem to be covered anymore since advanced combustion technology decreases the emissions of typical wood combustion markers (Czech et al., 2018). Although averages of obtained diagnostic ratios for primary and aged emissions appear in the same range, all ratios decreased with ageing, leading to significantly different means in a paired t-test. Hence, the diagnostic ratio of retene and chrysene is not valid for current wood combustion emissions, but offers potential to follow the aerosol age.

3.5.3. PAH toxicity equivalent emission factors

The concept of toxicity equivalents (TEQ) was firstly used for polychlorinated dibenzo-p-dioxins and polychlorinated dibenzofurans and eventually extended to PAH. It enables estimation of the potential of a mixture to induce cancer by multiplication of each detected PAH concentration or EF with its toxicity equivalent factor (TEF) and subsequent summation. In this concept, the well-investigated carcinogenicity of benz[a]pyrene is set to unity (Nisbet and LaGoy, 1992) and carcinogenicity of other PAH are set in relation. In the following, we refer to the TEF scale recommended by the German Research Foundation (Greim, 2008) (Table S3). In addition to primary and aged wood emissions, the PAH-TEQ of particulate emissions from a non-road diesel engine was added as reference for combustion emissions, which are carcinogenic to humans ("group 1" classification by IARC) (International Agency for Research on Cancer (IARC), 2019).

PAH-TEQ of primary spruce combustion aerosol, expressed as EF, covers a range from 11 to 230 µg MJ^{-1}, which is comparable to previously published PAH-TEQ of spruce logwood combustion in a wood stove (Orasche et al., 2012; Orasche et al., 2013). However, it is one order of magnitude higher than in combustion appliances with advanced combustion technology (Czech et al., 2018). Photochemical ageing, equivalent to 1.7 to 2.5 days, significantly decreased PAH-TEQ of the primary emissions by approximately one order of magnitude. Nevertheless, it remains two orders of magnitude higher than particulate emissions from a non-road diesel engine, a heavy-duty diesel truck on a US driving cycle and a burner operated on diesel-like light fuel oil (Fig. 6). From extrapolating the degradation of PAHs observed in this study to higher photochemical ages, we obtain that at least four days of photochemical ageing are necessary to reach the same PAH-TEQ level as primary diesel engine emissions.

PAH-TEQ allow a rough estimation of the carcinogenic potential after photochemical ageing. However, three basic aspects, which are in particular relevant for wood combustion emissions, are not considered. Firstly, emission constituents interact with each other and affect the total toxicity of an aerosol in both positive and negative directions. For example, on the one hand PAHs on wood

combustion particles induced expression of CYP1A1 more potently than benz[a]pyrene applied in suspension (Dilger et al., 2016). On the other hand, phenolic species are typical components of wood combustion aerosol and suspected to counteract oxidative processes in the human body by, e.g. scavenging reactive oxygen species, consequently decreasing oxidative stress or DNA modification (Kanashova et al., 2018; Kjällstrand and Petersson, 2001) during carcinogenesis. Moreover, it has been shown that the oxidative potential of particles comprised of naphthalene-SOA and copper is not additive (Wang et al., 2018). Secondly, PAHs are oxidised depending on reactants and radiation and largely transformed into OPAHs and nitro-PAHs, which are known for their carcinogenic effect on human health as well (Fu et al., 2012), but not taken into account by PAH-TEQ. The same holds for the heavy metals cadmium, chromium and nickel, which are also classified as carcinogenic to humans ("group 1") (International Agency for Research on Cancer (IARC), 2019) and found in similar concentration ranges as PAHs with five or more rings in wood combustion aerosol (Czech et al., 2018; Wiinikka et al., 2013). Finally, the particle size of the emission ultimately affects the location of deposition and point of action during human exposure for particle-bound carcinogens (Boström et al., 2002).

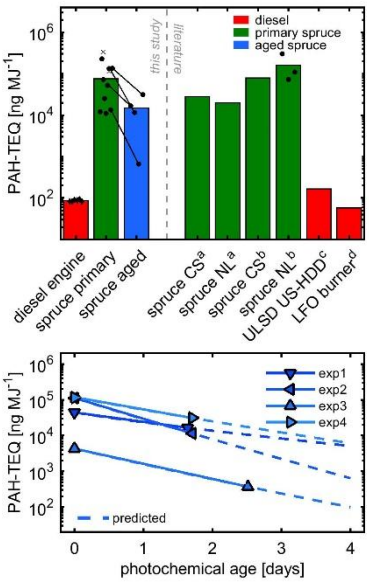

Fig. 6. Top: PAH-TEQ referred to benz[a]pyrene for primary (green) and aged (blue) spruce combustion emissions. Straight black lines denotes filter samples taken from primary and aged

aerosol of the same ageing experiment. PAH-TEQ from a diesel engine is included as reference for carcinogenic exhaust particles (red). Circles denote dilution ratio of 1:30 for filter sampling, while crosses show filter samples taken at 1:15 dilution (not included in the average values). Diesel emission filter samples were taken at 1:10 dilution ratio (diamonds). Literature data (right) was taken from (a) (Orasche et al., 2012), (b) (Orasche et al., 2013) (CS: cold start; NL: nominal load), (c) (Lin et al., 2011) (ULSD: ultra-low sulphur diesel; US-HDD: US engine cycle for heavy-duty diesel engines) and (d) (Kaivosoja et al., 2013) (LFO: diesel-like light fuel oil). Bottom: PAH-TEQ (solid lines) and extrapolated PAH-TEQ (dashed lines) with pseudo-first order kinetic constants derived from experiments exp1 to exp4 with 1.7 to 2.5 equivalent days of photochemical ageing (Fig. S4).

4. Conclusion

Primary emissions from spruce logwood combustion were aged in a new high-flow photochemical reactor (PEAR) with equivalent photochemical ages between 1.7 and 2.5 days in the atmosphere. OC increased by 26 to 43% due to SOA formation, while EC remained stable. In TOCA-REMPI analysis, a variety of aromatic species up to m/z of 400 was detected, including alkylation series of PAH and OPAH. Targeted analysis by IDTDGC-MS revealed 404 µg MJ^{-1} of 35 analysed PAH, 317 µg MJ^{-1} of 11 analysed Oxy-PAH and 12.5 µg MJ^{-1} of 5 analysed OH-PAH, emphasising the role of residential wood combustion as an important source of PAHs and OPAHs in the atmosphere. Photochemical ageing reduced the abundance of PAH by between 60 and 99% after 1.7 to 2.5 days of photochemical ageing, whereas Oxy-PAH decreased less due to their additional formation via photochemical reactions. In contrast, a substantial net increase of OH-PAH, in particular for 1,8-naphthaldehydic acid with a factor 36, was observed after ageing, which motivates further investigations on their relevance in toxicity of aged and ambient PM.

In both targeted and untargeted analysis, degradation of particle-bound aromatic compounds by photochemical ageing revealed minor differences between single aromatic species in contrast to

different reactivity of gas phase aromatics, Hence, further studies of PAHs and OPAHs degradation in aerosol emissions from different sources are necessary in order to derive cause-effect relations between properties of the substrate and photochemical decay of aromatic compounds.

PAHs have been widely used in diagnostic ratios to identify or to discriminate between wood combustion and other emissions sources. Phenanthrene/anthracene, fluoranthene/pyrene, retene/chrysene, and indeno[cd]pyrene/benzo[ghi]perylene were only slightly affected by photochemical ageing due to the general protection of particle-bound PAH by the particle composition and microstructure. In contrast, known degradation kinetics of benz[a]pyrene/benz[e]pyrene are sufficient to monitor atmospheric ageing of wood combustion aerosol. Moreover, the ratio of benz[a]anthracene/chrysene was also affected by ageing, despite similar reactivity towards OH. A possible explanation might be the higher importance of ozone as reactant, for which kinetic constants of benz[a]anthracene and chrysene differ by a factor of two.

The assessment of the carcinogenic potential of the wood combustion emission revealed that the PAH-TEQ is reduced by 45 to 80% per day of photochemical ageing. Nevertheless, photochemical ageing cannot be regarded as a process of net reducing carcinogenity of combustion aerosol due to parallel formation of other carcinogens, such as nitro-PAH. Hence, the toxicological effect of atmospheric ageing on combustion aerosols should be investigated in future studies by more sophisticated approaches, such as air-liquid exposure of lung cells followed by toxicological and multi-omics biological response analysis (Bauer et al., 2019; Kanashova et al., 2018; Oeder et al., 2015).

Acknowledgements

This research was funded by Academy of Finland (grants 296645 and 304459), Helmholtz Virtual Institute of Complex Molecular Systems in Environmental Health (HICE) by Helmholtz Impulse and

Network Fund of the Helmholtz Association (Germany), and the German Research Foundation (DFG) (grants ZI 764/5-1 and ZI 764/7-1).

References

Avagyan R, Nyström R, Lindgren R, Boman C, Westerholm R. Particulate hydroxy-PAH emissions from a residential wood log stove using different fuels and burning conditions. Atmos. Environ. 2016;140:1–9.

Bauer S, Happo MS, Abbaszade G, Adam T, Buters J, Candeias J et al. In vivo and in vitro toxicity of emissions from a stationary diesel generator. Sci. Total Environ. 2019;manuscript in preparation.

Bedjanian Y, Nguyen ML. Kinetics of the reactions of soot surface-bound polycyclic aromatic hydrocarbons with O3. Chemosphere 2010;79(4):387–93.

Behymer TD, Hites RA. Photolysis of Polycyclic Aromatic Hydrocarbons Adsorbed on Fly Ash. Environ. Sci. Technol. 1988;22(11):1311–9.

Boström C-E, Gerde P, Hanberg A, Jernström B, Johansson Cr, Kyrklund T et al. Cancer Risk Assessment, Indicators, and Guidelines for Polycyclic Aromatic Hydrocarbons in the Ambient Air. Environ. Health Perspect. 2002;110(s3):451–89.

Bruns EA, Krapf M, Orasche J, Huang Y, Zimmermann R, Drinovec L et al. Characterization of primary and secondary wood combustion products generated under different burner loads. Atmos. Chem. Phys. 2015;15(5):2825–41.

Chow JC, Watson JG, Chen L-WA, Chang MO, Robinson NF, Trimble D et al. The IMPROVE_A Temperature Protocol for Thermal/Optical Carbon Analysis: Maintaining Consistency with a Long-Term Database. J. Air Waste Manag. Assoc. 2007;57(9):1014–23.

Cordell RL, Mazet M, Dechoux C, Hama SML, Staelens J, Hofman J et al. Evaluation of biomass burning across North West Europe and its impact on air quality. Atmos. Environ. 2016;141:276–86.

Czech H, Miersch T, Orasche J, Abbaszade G, Sippula O, Tissari J et al. Chemical composition and speciation of particulate organic matter from modern residential small-scale wood combustion appliances. Sci. Total Environ. 2018;612:636–48.

Czech H, Sippula O, Kortelainen M, Tissari J, Radischat C, Passig J et al. On-line analysis of organic emissions from residential wood combustion with single-photon ionisation time-of-flight mass spectrometry (SPI-TOFMS). Fuel 2016;177:334–42.

Diab J, Streibel T, Cavalli F, Lee SC, Saathoff H, Mamakos A et al. Hyphenation of a EC / OC thermal–optical carbon analyzer to photo-ionization time-of-flight mass spectrometry: An off-line aerosol mass spectrometric approach for characterization of primary and secondary particulate matter. Atmos. Meas. Techn. 2015;8(8):3337–53.

Dilger M, Orasche J, Zimmermann R, Paur H-R, Diabaté S, Weiss C. Toxicity of wood smoke particles in human A549 lung epithelial cells: the role of PAHs, soot and zinc. Archives of Toxicology 2016;90(12):3029–44.

Eriksson AC, Nordin EZ, Nyström R, Pettersson E, Swietlicki E, Bergvall C et al. Particulate PAH emissions from residential biomass combustion: time-resolved analysis with aerosol mass spectrometry. Environ. Sci. Technol. 2014;48(12):7143–50.

Esteve W, Budzinski H, Villenave E. Relative rate constants for the heterogeneous reactions of OH, NO2 and NO radicals with polycyclic aromatic hydrocarbons adsorbed on carbonaceous particles.

Part 1: PAHs adsorbed on 1–2µm calibrated graphite particles. Atmos. Environ. 2004;38(35):6063–72.

Esteve W, Budzinski H, Villenave E. Relative rate constants for the heterogeneous reactions of NO2 and OH radicals with polycyclic aromatic hydrocarbons adsorbed on carbonaceous particles. Part 2: PAHs adsorbed on diesel particulate exhaust SRM 1650a. Atmos. Environ. 2006;40(2):201–11.

Evtyugina M, Alves C, Calvo A, Nunes T, Tarelho L, Duarte M et al. VOC emissions from residential combustion of Southern and mid-European woods. Atmos. Environ. 2014;83:90–8.

Ezell MJ, Johnson SN, Yu Y, Perraud V, Bruns EA, Alexander ML et al. A New Aerosol Flow System for Photochemical and Thermal Studies of Tropospheric Aerosols. Aerosol Sci. Technol. 2010;44(5):329–38.

Fine PM, Cass GR, Simoneit BRT. Chemical Characterization of Fine Particle Emissions from the Fireplace Combustion of Wood Types Grown in the Midwestern and Western United States. Environ. Eng. Sci. 2004;21(3):387–409.

Fu PP, Xia Q, Sun X, Yu H. Phototoxicity and environmental transformation of polycyclic aromatic hydrocarbons (PAHs)-light-induced reactive oxygen species, lipid peroxidation, and DNA damage. J. Environ. Sci. Health C Environ. Carcinog. Ecotoxicol. Rev. 2012;30(1):1–41.

Gaeggeler K, Prévôt ASH, Dommen J, Legreid G, Reimann S, Baltensperger U. Residential wood burning in an Alpine valley as a source for oxygenated volatile organic compounds, hydrocarbons and organic acids. Atmos. Environ. 2008;42(35):8278–87.

Galarneau E. Source specificity and atmospheric processing of airborne PAHs: Implications for source apportionment. Atmos. Environ. 2008;42(35):8139–49.

Gehm C, Streibel T, Passig J, Zimmermann R. Determination of Relative Ionization Cross Sections for Resonance Enhanced Multiphoton Ionization of Polycyclic Aromatic Hydrocarbons. Appl. Sci. 2018;8(9):1617.

Glasius M, Hansen AMK, Claeys M, Henzing JS, Jedynska AD, Kasper-Giebl A et al. Composition and sources of carbonaceous aerosols in Northern Europe during winter. Atmos. Environ. 2018;173:127–41.

Grabowsky J, Streibel T, Sklorz M, Chow JC, Watson JG, Mamakos A et al. Hyphenation of a carbon analyzer to photo-ionization mass spectrometry to unravel the organic composition of particulate matter on a molecular level. Anal. Bioanal. Chem. 2011;401(10):3153–64.

Greim H. Gesundheitsschädliche Arbeitsstoffe - Toxikologisch-arbeitsmedizinische Begründungen von MAK-Werten und Einstufungen: Wiley-VCH; 2008.

Hovorka J, Pokorná P, Hopke PK, Křůmal K, Mikuška P, Píšová M. Wood combustion, a dominant source of winter aerosol in residential district in proximity to a large automobile factory in Central Europe. Atmos. Environ. 2015;113:98–107.

Ihalainen M, Tiitta P, Czech H, Yli-Pirilä P, Hartikainen A, Kortelainen M et al. A novel high-volume Photochemical Emission Aging flow tube Reactor (PEAR). Aerosol Sci. Technol. 2019;53(3):276–94.

International Agency for Research on Cancer (IARC). List of Classifications, Volumes 1-123, 2019. https://monographs.iarc.fr/wp-content/uploads/2019/02/List_of_Classifications.pdf.

Jariyasopit N, Zimmermann K, Schrlau J, Arey J, Atkinson R, Yu T-W et al. Heterogeneous reactions of particulate matter-bound PAHs and NPAHs with NO3/N2O5, OH radicals, and O3 under simulated long-range atmospheric transport conditions: reactivity and mutagenicity. Environ. Sci. Technol. 2014;48(17):10155–64.

Kaivosoja T, Jalava PI, Lamberg H, Virén A, Tapanainen M, Torvela T et al. Comparison of emissions and toxicological properties of fine particles from wood and oil boilers in small (20–25 kW) and medium (5–10 MW) scale. Atmos. Environ. 2013;77:193–201.

Kamens RM, Guo Z, Fulcher JN, Bell DA. The influence of humidity, sunlight, and temperature on the daytime decay of polyaromatic hydrocarbons on atmospheric soot particles. Environ. Sci. Technol. 1988;22(1):103–8.

Kamens RM, Karam H, Guo J, Perry JM, Stockburger L. The behavior of oxygenated polycyclic aromatic hydrocarbons on atmospheric soot particles. Environ. Sci. Technol. 1989;23(7):801–6.

Kanashova T, Sippula O, Oeder S, Streibel T, Passig J, Czech H et al. Emissions from a Modern Log wood Masonry Heater and Wood Pellet Boiler: Composition and Biological Impact on Air-Liquid Interface Exposed Human Lung Cancer Cells. J. Mol. Clin. Med. 2018;1:23–35.

Kasurinen S, Jalava PI, Happo MS, Sippula O, Uski O, Koponen H et al. Particulate emissions from the combustion of birch, beech, and spruce logs cause different cytotoxic responses in A549 cells. Environ. Toxicol. 2017;32(5):1487–99.

Keller A, Burtscher H. A continuous photo-oxidation flow reactor for a defined measurement of the SOA formation potential of wood burning emissions. J. Aersosol Sci. 2012;49:9–20.

Keyte IJ, Albinet A, Harrison RM. On-road traffic emissions of polycyclic aromatic hydrocarbons and their oxy- and nitro- derivative compounds measured in road tunnel environments. Sci. Total Environ. 2016;566-567:1131–42.

Keyte IJ, Harrison RM, Lammel G. Chemical reactivity and long-range transport potential of polycyclic aromatic hydrocarbons--a review. Chem. Soc. Rev. 2013;42(24):9333–91.

Kjällstrand J, Petersson G. Phenolic antioxidants in wood smoke. Sci. Total Environ. 2001;277(1-3):69–75.

Kortelainen M, Jokiniemi J, Nuutinen I, Torvela T, Lamberg H, Karhunen T et al. Ash behaviour and emission formation in a small-scale reciprocating-grate combustion reactor operated with wood chips, reed canary grass and barley straw. Fuel 2015;143:80–8.

Künzi L, Mertes P, Schneider S, Jeannet N, Menzi C, Dommen J et al. Responses of lung cells to realistic exposure of primary and aged carbonaceous aerosols. Atmos. Environ. 2013;68:143–50.

Lamberg H, Nuutinen K, Tissari J, Ruusunen J, Yli-Pirilä P, Sippula O et al. Physicochemical characterization of fine particles from small-scale wood combustion. Atmos. Environ. 2011;45(40):7635–43.

Lamberg H, Tissari J, Jokiniemi J, Sippula O. Fine Particle and Gaseous Emissions from a Small-Scale Boiler Fueled by Pellets of Various Raw Materials. Energy Fuels 2013;27(11):7044–53.

Li M, Bao F, Zhang Y, Song W, Chen C, Zhao J. Role of elemental carbon in the photochemical aging of soot. Proc. Natl. Acad. Sci. U.S.A. 2018;115(30):7717–22.

Lin Y-C, Hsu K-H, Chen C-B. Experimental investigation of the performance and emissions of a heavy-duty diesel engine fueled with waste cooking oil biodiesel/ultra-low sulfur diesel blends. Energy 2011;36(1):241–8.

Naeher LP, Brauer M, Lipsett M, Zelikoff JT, Simpson CD, Koenig JQ et al. Woodsmoke health effects: a review. Inhal. Toxicol. 2007;19(1):67–106.

Nisbet ICT, LaGoy PK. Toxic equivalency factors (TEFs) for polycyclic aromatic hydrocarbons (PAHs). Regul. Toxicol. Pharmacol. 1992;16(3):290–300.

Nordin EZ, Uski O, Nyström R, Jalava P, Eriksson AC, Genberg J et al. Influence of ozone initiated processing on the toxicity of aerosol particles from small scale wood combustion. Atmos. Environ. 2015;102:282–9.

Nuopponen MH, Birch GM, Sykes RJ, Lee SJ, Stewart D. Estimation of wood density and chemical composition by means of diffuse reflectance mid-infrared Fourier transform (DRIFT-MIR) spectroscopy. J. Agric. Food Chem. 2006;54(1):34–40.

Nuutinen K, Jokiniemi J, Sippula O, Lamberg H, Sutinen J, Horttanainen P et al. Effect of air staging on fine particle, dust and gaseous emissions from masonry heaters. Biomass Bioenergy 2014;67:167–78.

Nyström R, Lindgren R, Avagyan R, Westerholm R, Lundstedt S, Boman C. Influence of Wood Species and Burning Conditions on Particle Emission Characteristics in a Residential Wood Stove. Energy Fuels 2017;31(5):5514–24.

Oeder S, Kanashova T, Sippula O, Sapcariu SC, Streibel T, Arteaga-Salas JM et al. Particulate matter from both heavy fuel oil and diesel fuel shipping emissions show strong biological effects on human lung cells at realistic and comparable in vitro exposure conditions. PLOS ONE 2015;10(6):e0126536.

Oliveira C, Martins N, Tavares J, Pio C, Cerqueira M, Matos M et al. Size distribution of polycyclic aromatic hydrocarbons in a roadway tunnel in Lisbon, Portugal. Chemosphere 2011;83(11):1588–96.

Orasche J, Schnelle-Kreis J, Abbaszade G, Zimmermann R. Technical Note: In-situ derivatization thermal desorption GC-TOFMS for direct analysis of particle-bound non-polar and polar organic species. Atmos. Chem. Phys. 2011;11(17):8977–93.

Orasche J, Schnelle-Kreis J, Schön C, Hartmann H, Ruppert H, Arteaga-Salas JM et al. Comparison of Emissions from Wood Combustion. Part 2: Impact of Combustion Conditions on Emission Factors and Characteristics of Particle-Bound Organic Species and Polycyclic Aromatic Hydrocarbon (PAH)-Related Toxicological Potential. Energy Fuels 2013;27(3):1482–91.

Orasche J, Seidel T, Hartmann H, Schnelle-Kreis J, Chow JC, Ruppert H et al. Comparison of Emissions from Wood Combustion. Part 1: Emission Factors and Characteristics from Different Small-Scale Residential Heating Appliances Considering Particulate Matter and Polycyclic Aromatic Hydrocarbon (PAH)-Related Toxicological Potential of Particle-Bound Organic Species. Energy Fuels 2012;26:6695−6704.

Palm BB, Campuzano-Jost P, Ortega AM, Day DA, Kaser L, Jud W et al. In situ secondary organic aerosol formation from ambient pine forest air using an oxidation flow reactor. Atmos. Chem. Phys. 2016;16(5):2943–70.

Peng Z, Day DA, Ortega AM, Palm BB, Hu W, Stark H et al. Non-OH chemistry in oxidation flow reactors for the study of atmospheric chemistry systematically examined by modeling. Atmos. Chem. Phys. 2016;16(7):4283–305.

Peng Z, Jimenez JL. Modeling of the chemistry in oxidation flow reactors with high initial NO. Atmos. Chem. Phys. 2017;17(19):11991–2010.

Pieber SM, Kumar NK, Klein F, Comte P, Bhattu D, Dommen J et al. Gas-phase composition and secondary organic aerosol formation from standard and particle filter-retrofitted gasoline direct injection vehicles investigated in a batch and flow reactor. Atmos. Chem. Phys. 2018;18(13):9929–54.

Pio C, Cerqueira M, Harrison RM, Nunes T, Mirante F, Alves C et al. OC/EC ratio observations in Europe: Re-thinking the approach for apportionment between primary and secondary organic carbon. Atm. Environ. 2011;45(34):6121–32.

Prinn RG, Huang J, Weiss RF, Cunnold DM, Fraser PJ, Simmonds PG et al. Evidence for Substantial Variations of Atmospheric Hydroxyl Radicals in the Past Two Decades. Science 2001;292(5523):1876–82.

Qadir RM, Schnelle-Kreis J, Abbaszade G, Arteaga-Salas JM, Diemer J, Zimmermann R. Spatial and temporal variability of source contributions to ambient PM10 during winter in Augsburg, Germany using organic and inorganic tracers. Chemosphere 2014;103:263–73.

Ravindra K, Sokhi R, van Grieken R. Atmospheric polycyclic aromatic hydrocarbons: Source attribution, emission factors and regulation. Atmos. Environ. 2008;42(13):2895–921.

Reche C, Viana M, Amato F, Alastuey A, Moreno T, Hillamo R et al. Biomass burning contributions to urban aerosols in a coastal Mediterranean city. Sci. Total Environ. 2012;427-428:175–90.

Simoneit BRT. Biomass burning — a review of organic tracers for smoke from incomplete combustion. Applied Geochemistry 2002;17(3):129–62.

Sippula O, Lamberg H, Leskinen J, Tissari J, Jokiniemi J. Emissions and ash behavior in a 500 kW pellet boiler operated with various blends of woody biomass and peat. Fuel 2017;202:144–53.

Tkacik DS, Lambe AT, Jathar S, Li X, Presto AA, Zhao Y et al. Secondary organic aerosol formation from in-use motor vehicle emissions using a potential aerosol mass reactor. Environ. Sci. Technol. 2014;48(19):11235–42.

Tobiszewski M, Namieśnik J. PAH diagnostic ratios for the identification of pollution emission sources. Einviron. Pollut. 2012;162:110–9.

Vione D, Maurino V, Minero C, Pelizzetti E, Harrison MAJ, Olariu R-I et al. Photochemical reactions in the tropospheric aqueous phase and on particulate matter. Chem. Soc. Rev. 2006;35(5):441–53.

Walgraeve C, Demeestere K, Dewulf J, Zimmermann R, van Langenhove H. Oxygenated polycyclic aromatic hydrocarbons in atmospheric particulate matter: Molecular characterization and occurrence. Atmos. Environ. 2010;44(15):1831–46.

Wang S, Ye J, Soong R, Wu B, Yu L, Simpson AJ et al. Relationship between chemical composition and oxidative potential of secondary organic aerosol from polycyclic aromatic hydrocarbons. Atmos. Chem. Phys. 2018;18(6):3987–4003.

Wiinikka H, Grönberg C, Boman C. Emissions of Heavy Metals during Fixed-Bed Combustion of Six Biomass Fuels. Energy Fuels 2013;27(2):1073–80.

Yan B, Abrajano TA, Bopp RF, Chaky DA, Benedict LA, Chillrud SN. Molecular Tracers of Saturated and Polycyclic Aromatic Hydrocarbon Inputs into Central Park Lake, New York City. Environ. Sci. Technol. 2005;39(18):7012–9.

Highlights

- targeted and untargeted analysis of aromatics in primary and aged wood combustion PM2.5
- reassessment of PAH diagnostic ratios for source identification
- Oxy-PAH were less degraded by photochemical ageing than PAH
- increase of OH-PAH during photochemical ageing
- PAH-TEQ reduced by 90% after two days of photochemical ageing